

Alumina, Hiperco-50 and Boron Nitride Xe⁺ Sputter Yields

IEPC-2017-17

35th International Electric Propulsion Conference, Atlanta, GA

October 8-12, 2017

Mark W. Crofton¹ and Jason A. Young²

The Aerospace Corporation, El Segundo, CA, 90245, United States

Abstract: Electric thruster materials are often subject to erosion during normal device operation. As a result of the ion sputtering process surface properties can be affected or underlying material may be exposed, possibly compromising performance and/or lifetime. It is therefore important to know both the energy and angle dependence of total sputter yield (TSY) for relevant materials, so these effects can be predicted. In this study we have obtained limited data sets on three materials with applications to electric propulsion and spacecraft - alumina, Hiperco 50 and HP boron nitride, in order to augment the material properties database. For each case angular profiles were obtained at a single ion incidence energy and energy dependence was explored at normal incidence. These materials find application in other technological areas as well.

¹ Senior Scientist, Propulsion Science Department, mark.w.crofton@aero.org

² Member of the Technical Staff, Propulsion Science Department, jason.a.young@aero.org

I. Introduction

Electric propulsion devices based on ion emission for thrust generation can cause erosion and deposition that impact performance and lifetime, as well as integration issues for the spacecraft that use them. Metal and insulator atoms and ions produced via sputter erosion may find their way into the plume and deposit on spacecraft surfaces, modifying their properties. Due to the inherent divergence of the ion beam there may be intercepted surfaces that undergo sputter erosion, modifying roughness, composition, and thickness. Erosion and deposition processes inside thrusters potentially modify the lifetime potential as well. Plume density and flux depend on angle with respect to the thrust axis, thruster operating point, composition of components, and facility background pressure. Net mass deposition rates are also a function of ion beam flux, due to simultaneous removal of depositing species, and the ion beam flux varies sharply with angle.

Sputter rate depends strongly on the kinetic energy, incident angle and identity of the ion. Therefore it is necessary to measure the sputter yield as a function of these parameters. Xenon is the baseline propellant for ion propulsion, with krypton as an alternative. Xe^+ is therefore the main ion of interest for sputter yield measurements in the ion propulsion field.

For the present study several materials of interest were selected for which sputter data have been lacking. Hiperc 50 is a soft magnetic alloy of essentially equal parts cobalt and iron at 49% each, and 2% vanadium. Trace amounts of niobium, silicon and manganese are present as well. It has the highest magnetic saturation (24 kilogauss) of any commercial alloy, and its permeability is quite high also. The Curie temperature is 940C and melting point is 1427C. No sputter yield measurements were found in the literature for Hiperc 50, which is also known as Permendur. The varieties Hiperc 50 and 50A are nearly identical. Among Hiperc properties of interest are temperature dependence of magnetic field strength and Xe^+ sputter yield.

Alumina (Al_2O_3) is one of the most widely used engineering ceramics. One use is as a pole piece coating.¹ It exhibits excellent chemical resistance even at elevated temperature. It is a very good electrical insulator, with moderate thermal conductivity. While its energy-dependent sputter yield has previously been evaluated for normal incidence Xe^+ ,¹ no angle-dependent sputter yield measurements were found in the literature.

Hall thruster discharge channels are often made of some type of boron nitride material. Its composition is more complex and variable than the other materials included in the present study, and it tends to absorb significant amounts of atmospheric water. The potential formation of gaseous species like molecular nitrogen during the erosion/deposition process means that some sputtered atoms may be underrepresented in the deposition layer on a monitoring quartz crystal microbalance. Robust absorption of atmospheric water vapor similarly can compromise the accuracy of weight measurements for obtaining sputter yield results. In addition, BN physical properties can vary significantly, such that samples assumed to be identical may absorb water vapor differently² and might even differ in fundamental properties like density. The effects of plasma exposure present a further complication, with the type of exposure further modifying physical properties such as roughness and sputter yield. While roughness itself is well known to be a sputter yield modifier³ plasma exposure may intrinsically modify sputter yield even if roughness is little affected.^{4,5} As a result, literature results may be unreliable. Properties will also depend on the particular type of BN selected for the measurement; for the present study HP grade boron nitride is used and results are compared only to HP literature results.

II. Experimental

A 3-cm diameter Commonwealth Scientific gridded ion source provided ions of variable kinetic energy for the sputter yield measurements. The grids were made of carbon rather than molybdenum to reduce the sample deposition flux from eroding grid material.

Base pressure established by the test facility with no xenon flow through the neutralizer cathode or 3-cm ion source was 5×10^{-8} torr. A constant xenon background pressure of about 2.4×10^{-6} torr was present when both of these devices were operating normally. A single TM1200i internal cryopump was the only active vacuum pump during the measurements, and its pumping speed was about 30 kltr/s for xenon.

A diagram of the experimental configuration is shown in Figure 1, with photographs provided in Figures 2 and 3. Molybdenum samples at 0, 30, 55, and 75 degrees angle of incidence (AOI), biased at -18V, were used for ion current data collection. These were obtained from ESPI metals, with 3N8 purity (99.98%). Molybdenum sample size was about 3.81 cm square, and current was measured in each case via the voltage drop across a 1 kilo ohm resistor using a Stanford Research Systems SR630 thermocouple monitor. Figure 4 has example plots of collected ion current vs incident ion energy and vs molybdenum collector AOI. The angular dependence varies as $\cos \theta$ to good approximation,

with small deviations due to slight errors in mounting angle and source to collector distance. At 250 eV the achievable ion collection was much lower than is readily obtained at ≥ 500 eV.

Sample size in each case was 3.785 cm square, with machined corner mounting holes. High density samples were less than 0.25-mm thick for low weight. The Al_2O_3 samples were alpha phase procured from Questek with 99.6% purity⁶, average grain size > 1 micron, surface roughness center line average >25 nm as-fired, 3.87 g/cm^3 density and 0.50-mm thickness. Water absorption and gas permeability were very low according to the supplier. Mounting holes were laser machined.

Hiperco 50 samples were 0.178-mm thick and procured from Ed Fagan. In addition to about 49% each of iron and cobalt, these samples contained 1.9% vanadium, 0.19% nickel, 0.09% chromium, 0.06% niobium, 0.04% silicon, and trace levels of manganese, phosphorus, and sulfur. The BN samples were procured from Saint Gobain. The material is HP grade, a hexagonal hot pressed boron nitride with calcium borate binder. HP elemental composition has been reported to be 92% BN, 3% calcium, and about 5% $\text{B}(\text{OH})_3$ with trace levels of B_2O_3 . [SATONIK] Samples used in the present study were certified as 2.6% calcium, 5.2% oxygen, 0.42% B_2O_3 , 0.22% silicon, and 0.016% magnesium, plus trace levels of several other elements. Specified sample density was 2.03 g/cm^3 density. A second group of HP grade samples obtained from the same supplier and not utilized for the present study, had density of 2.01 g/cm^3 and certified composition with, for example, just 2.3% calcium. Samples were weighed before and after ion exposures on a Sartorius MC5 balance with 5.1 gram limit and $1 \mu\text{g}$ readability. Because the sample weight varied with room temperature and relative humidity, especially for the boron nitride, samples were always acclimated to the balance room for at least 24 hours and two control samples for each material type were included. Because the room temperature and humidity was not tightly controlled, those variations could still affect the weighing accuracy. The difference with respect to control mass was used before and after exposures to determine the sample mass change. Control samples were not exposed to the ion beam or chamber vacuum during the test sequence. A radioisotope mounted on the weighing chamber emitted alpha particles to minimize electrostatic charge level during the measurements.

Samples were weighed before and after ion beam exposures, following the acclimation period. The alumina samples appeared to absorb a small amount of atmospheric water vapor, stabilizing in ≤ 5 minutes on the balance. Day to day reproducibility was good. Hiperco samples were rotated by 90 degrees on the balance, up to 360, and weight readings averaged; due to residual magnetization in the material this was necessary to obtain appropriate mass figures.

Both angular dependence (at 350 eV) and energy dependence were studied. Angular dependence was measured at 0, 30, 45, 55, 65, and 75 degrees. Test methodology was validated via comparison of molybdenum TSY measurement results to literature values. TSY results for these complex materials are presented in terms of volumetric loss per Coulomb of incident ions (mm^3/C units).

Since collection current varied with ion energy and AOI, and sample roughness was modified during exposures, exposure times were adjusted to produce more consistent thickness change than would otherwise be the case. The 250 eV exposure naturally had the lowest thickness change because it was not practical to expose long enough to fully compensate for the low ion beam current and sputter yield in that instance. An example plot of the computed thickness changes for alumina samples during the various exposures is given in Figure 5, showing approximately $\times 2$ variation if the 250 eV case is excluded.

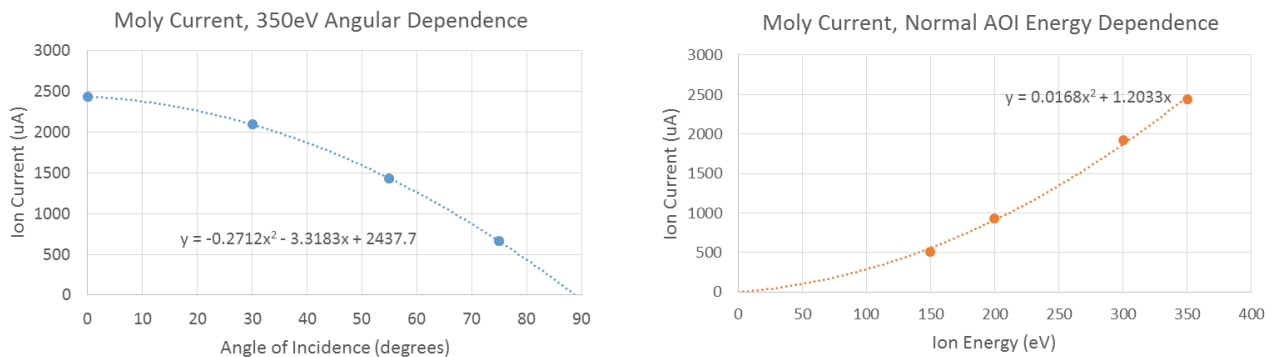


Figure 1. Molybdenum ion collection current as a function of Xe^+ AOI at fixed 350 eV (left) and impingement energy at 0 degrees AOI (right).

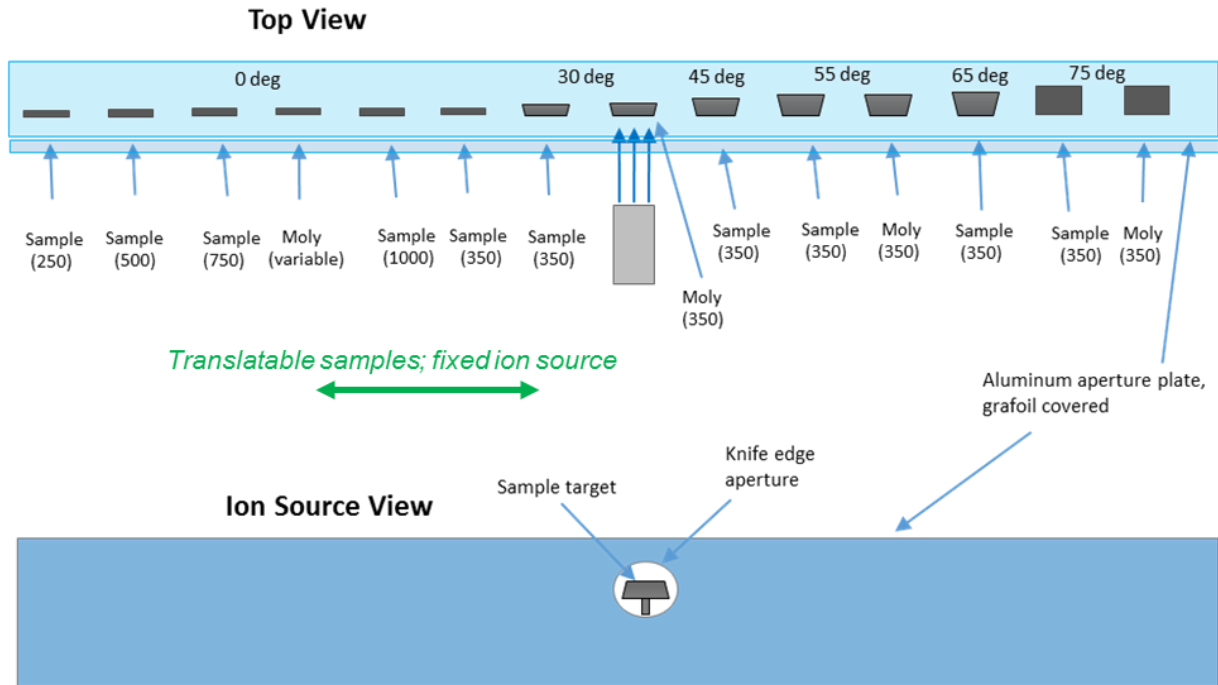


Figure 2. Overall sputter yield measurement setup. The samples are mounted on a large moveable stage containing an aperture, so that samples can be sequentially exposed. Each moly target is electrically connected to an external instrument for measuring collection current and charge fluence.

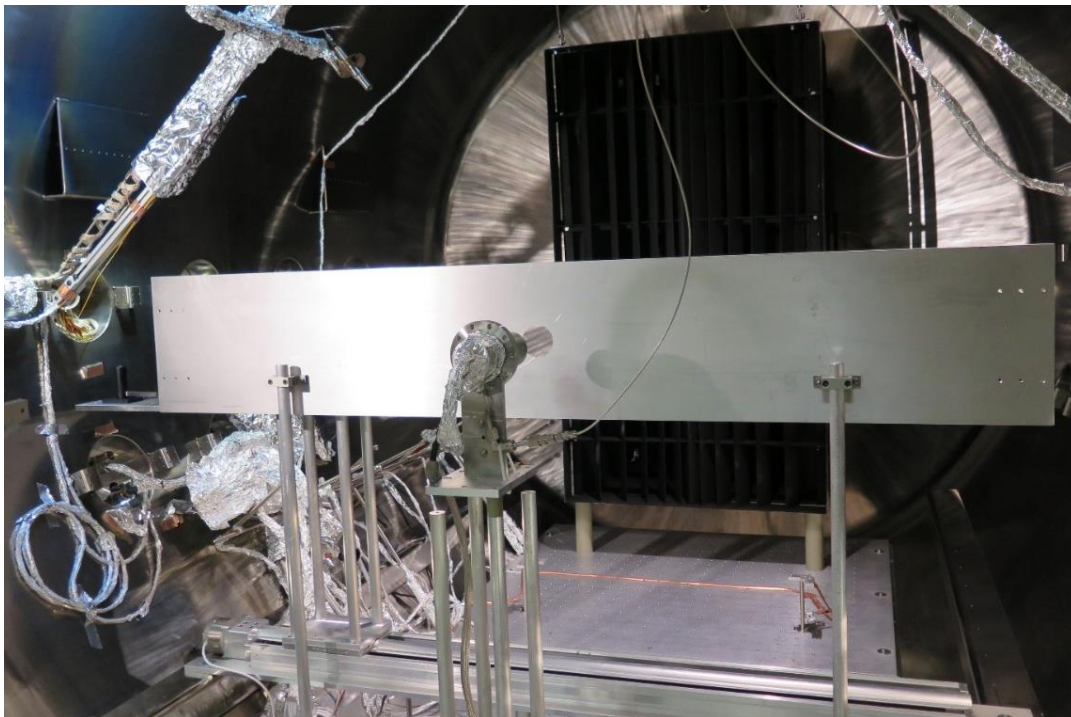


Figure 3. Photo from behind the ion source and aperture plate. Samples are mounted on the other side of the plate. A hollow cathode (plasma bridge) neutralizer located above and to the left keeps the ion beam and samples at low electric potential.

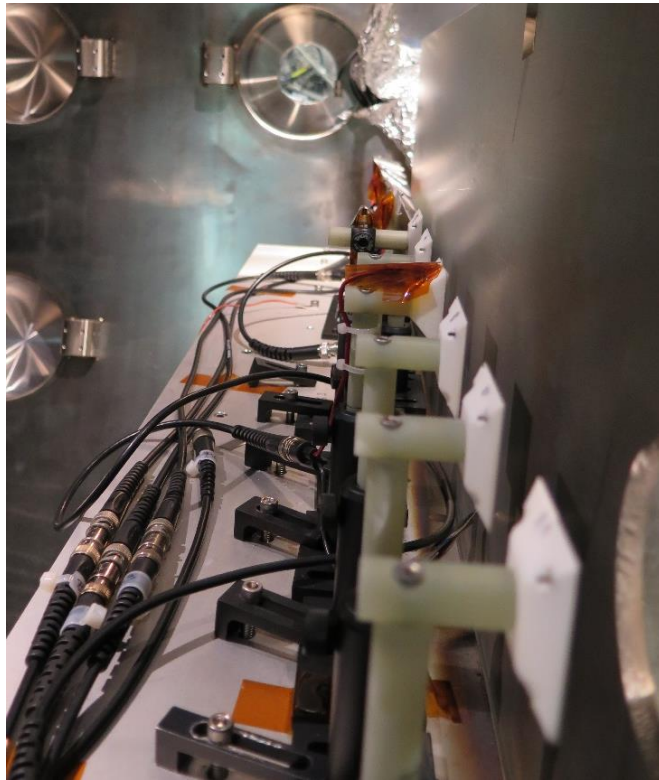


Figure 4. Photo of the line-up of sputter target and current collector holders for the exposure sequence.

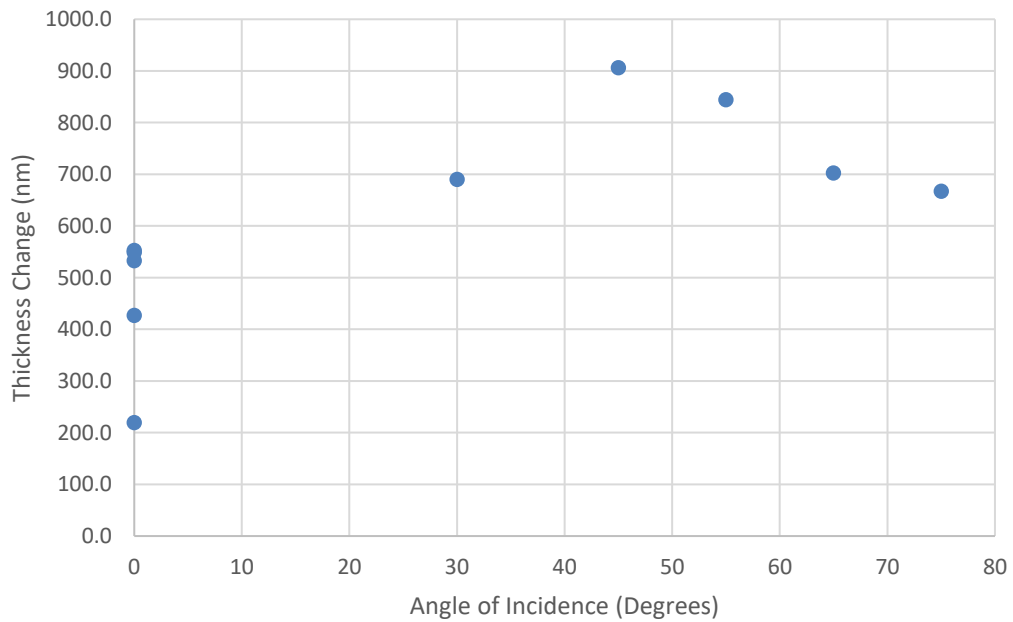


Figure 5. Absolute magnitude of thickness change for Al_2O_3 samples based on weight loss measurements (the change during sample exposures was negative).

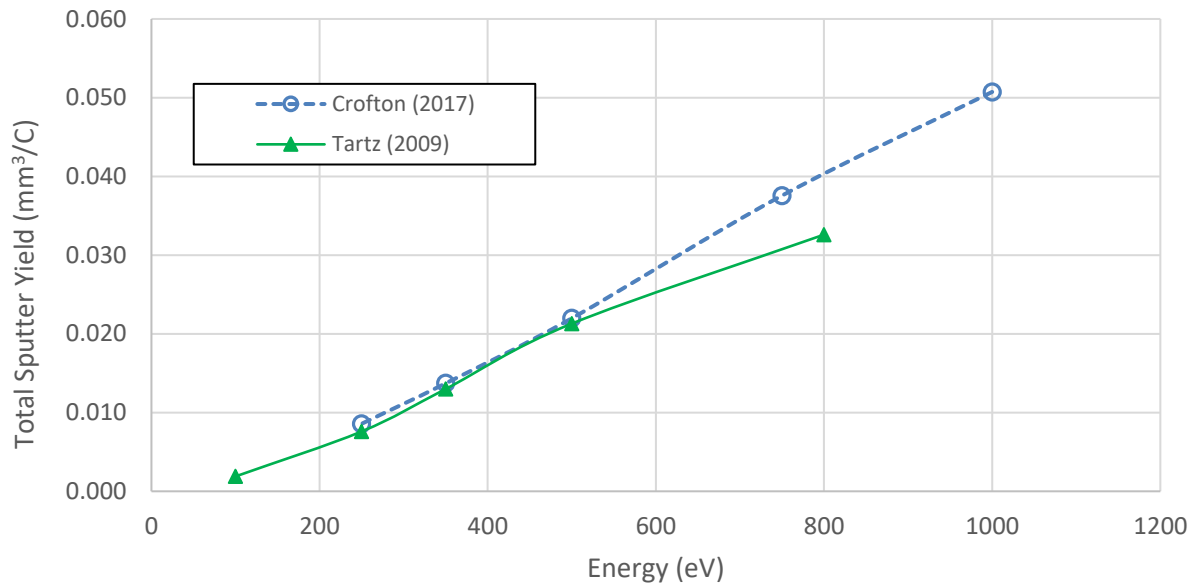


Figure 6. Dependence of measured Al_2O_3 total sputter yield on Xe^+ impingement energy at normal incidence.

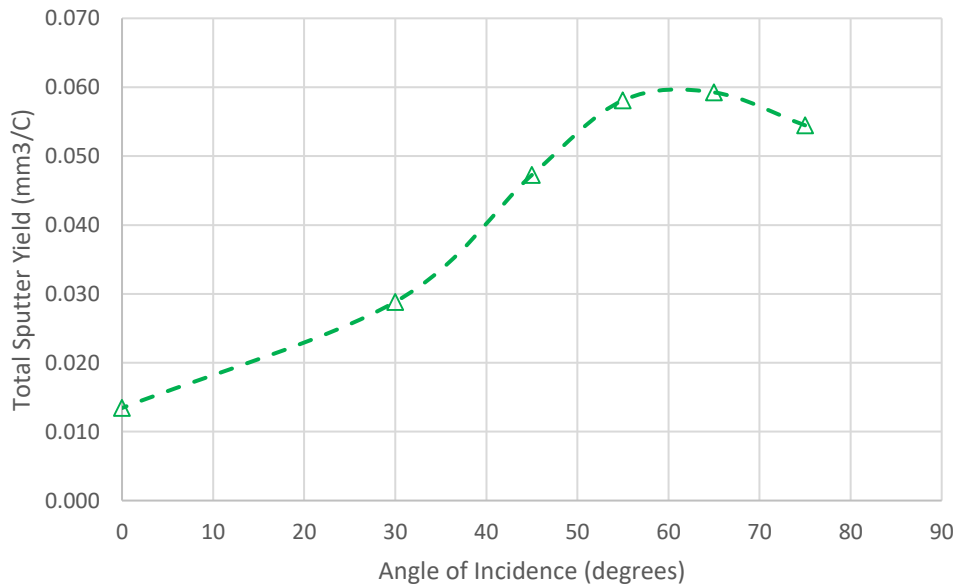


Figure 7. Dependence of measured Al_2O_3 total sputter yield on angle of incidence, for 350 eV Xe^+ ions.

III. Results and Discussion

A. Alumina

The measured alumina TSY energy dependence found by the present study is plotted in Figure 6, together with the only other measurement result found in the literature.⁷ These volumetric results compare extremely well in the 250 – 500 eV energy range, strongly suggesting they are accurate. For energy on the high side of this range there is a

modest discrepancy, the reason for which is unknown. The angular dependence, measured here for the first time, is given in Figure 7. A very smooth yield profile can be drawn through the data points, indicating low scatter and a high degree of internal consistency. The peak position is observed to be close to 60 degrees, with $\sim 4.5:1$ ratio between the peak and 0-degree AOI.

B. Hiperco 50

Energy dependence of the Hiperco 50 volumetric TSY is presented in Figure 8. For the same energy the TSY is about $3\times$ higher than alumina. With its $\sim 2\times$ higher density Hiperco mass change is much greater for an identical exposure. Like alumina the data exhibit low scatter, suggesting high accuracy. The measured angular dependence is

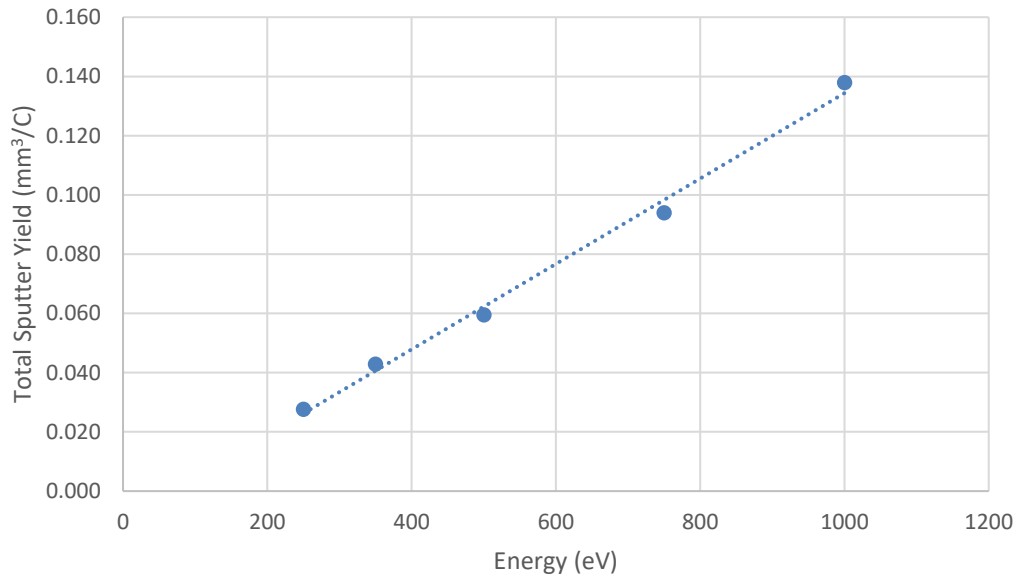


Figure 8. Dependence of measured Hiperco 50 total sputter yield on ion impingement energy.

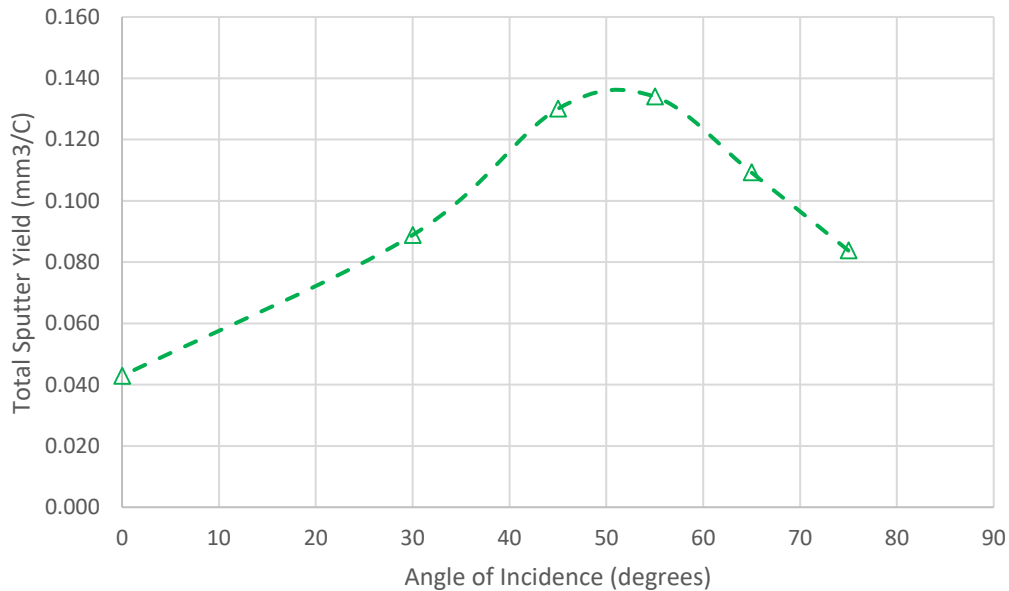


Figure 9. Dependence of measured Hiperco 50 total sputter yield on angle of incidence, for 350 eV Xe^+ ions.

plotted in Figure 9. Here TSY peaks at about 50 degrees AOI, lower than found for alpha phase alumina. As was the case for Al_2O_3 , all of the Hiperco data exhibit low scatter and a high degree of internal consistency.

C. HP Grade Boron Nitride

Energy dependent TSY for HP grade BN is plotted in Figure 10, together with literature HP results for comparison. Rubin et al² obtained their results from QCM measurements of condensable material and scaled TSY up to account for undetected volatile species. The Tartz results⁷ were obtained via weight loss measurements, and are in much better agreement with the present study, particularly in the 250 – 500 eV regime. For HP the TSY data obtained by Tartz et al⁷ at higher energy lie significantly below our results, just as in the case of alumina, and seem to agree better at lower energy.

Measured TSY angular dependence is plotted in Figure 11. Here the profile is much more flat with respect to angle than observed with alumina and Hiperco, and combined with greater uncertainty with respect to the true value of any particular data point it is difficult to ascertain the correct profile. BN is similar to graphite in its condensed phase structure; at low energy graphite can also exhibit little TSY angular dependence. Based on the amount of scatter in the HP data compared to alumina and Hiperco, the BN results are clearly less accurate but not excessively so.

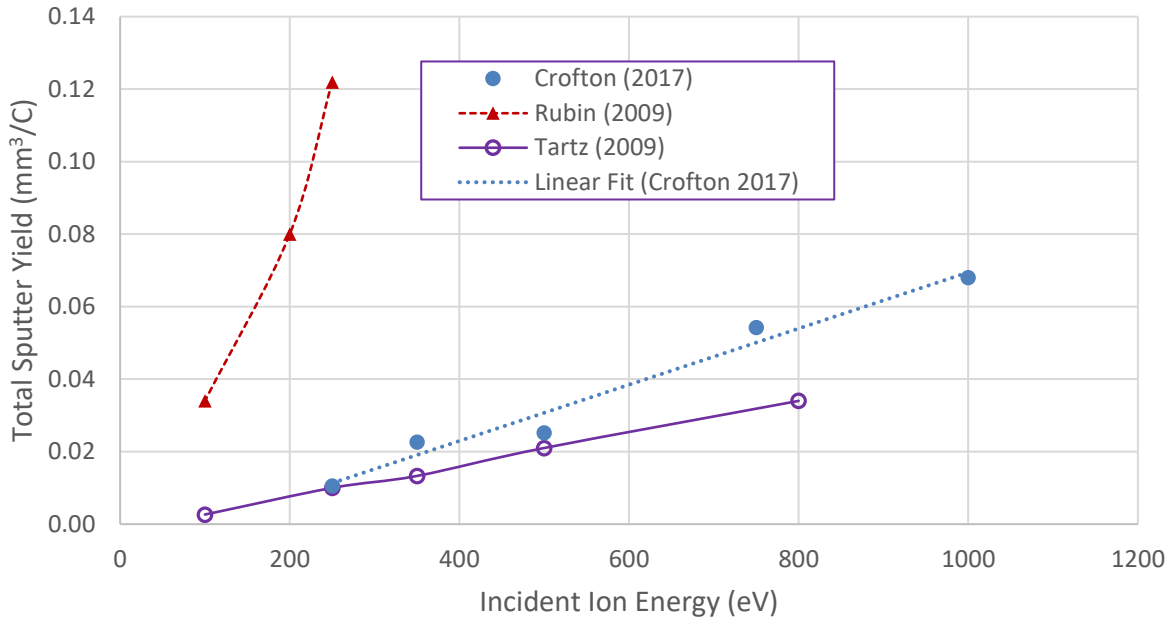


Figure 10. HP grade boron nitride energy dependence at 0 degrees, comparing current study results with literature values.

IV. Discussion

A variety of small corrections are possible but have not been made to these data. The largest sources of uncertainty are expected to be in the Xe^+ fluence measurement and TSY variation with evolving surface condition - roughness in particular,³ and atmospheric absorption effects which were very significant for boron nitride^{2,7} and relatively minor for alumina and Hiperco. Another significant factor is the width of the ion source energy distribution at beam energy of 250 eV and below. If the effect of surface condition is ignored, for favorable alumina and Hiperco cases with respect to current measurement, TSY accuracy better than 10% can be expected.

At normal incidence Hiperco TSY was about 3× higher than alumina over the 250 – 1000 eV energy range investigated and twice higher than the boron nitride. Alumina exhibited the greatest 350 eV angular dependence with Hiperco second. Boron nitride showed strong energy dependence but there was little angular effect at the tested energy.

The angular enhancement factor (ratio of peak angular TSY to normal incidence value) for alumina at 350 eV was determined to be about 4.5, approximately 50% larger than modeled by Ortega et al.¹ Angular enhancement depends on the material as well as incident energy. It trends higher with ion energy.

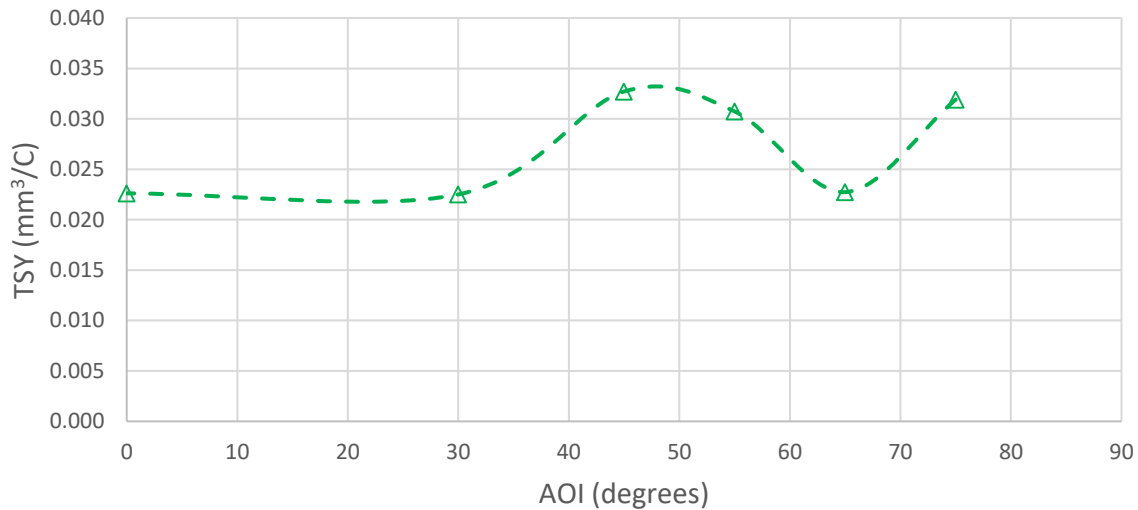


Figure 11. Total sputter yield angular dependence of HP boron nitride at 350 eV Xe⁺ impingement energy. Due to measurement uncertainty the precise shape of the profile is unknown.

V. Conclusion

Total Xe⁺ sputter yield has been measured for alumina, Hiperco 50 and HP grade boron nitride, important materials for electric space propulsion and other applications. For alumina no prior published results on Xe⁺ angular dependence were found, and no prior energy or angular measurements were found for Hiperco 50. Energy dependence was studied at normal incidence and angular dependence at fixed 350 eV ion energy. Alumina and Hiperco data were well behaved, with boron nitride results exhibiting much more scatter – indicating that this material is unusual in its behavior. High variability is a key feature of boron nitride literature results, and individual samples were found to respond in different ways to the presence of atmospheric water vapor – strongly suggesting that pre-exposure samples cannot be considered equivalent. Knowledge of the starting surface condition and its evolution during sputter measurements is useful to fully understand implications of the data, and is of interest for future work with all of the materials included in this study.

At normal incidence Hiperco TSY was about 3× higher than alumina over the 250 – 1000 eV energy range investigated and twice higher than the boron nitride. Alumina exhibited the greatest 350 eV angular dependence with Hiperco second. Boron nitride showed strong energy dependence but there was little angular effect at the tested energy.

The angular enhancement factor (ratio of peak angular TSY to normal incidence value) for alumina at 350 eV was determined to be about 4.5, approximately 50% larger than modeled by Ortega et al.¹ Angular enhancement depends on the material as well as incident energy. It trends higher with ion energy.

VI. Acknowledgments

This project was supported under The Aerospace Corporation’s Independent Research and Development Program. The authors thank Michael J. Patterson of NASA Glenn Research Center for valuable assistance with setup of the ion beam neutralization system, and De-Ling Liu for use of the microbalance.

References

1. A.L. Ortega, B.A. Jorns, I.G. Mikellides and R.R. Hofer, "Numerical Simulations of the XR-5 Hall Thruster for Life Assessment at Different Operating Conditions," AIAA Paper 2015-4008, Orlando, July 2015.
2. B. Rubin, J.L. Topper and A.P. Yalin, "Total and Differential Sputter Yields of Boron Nitride Measured by Quartz Crystal Microbalance," *J. Phys. D: Appl. Phys.* **42**, 205205 (2009).
3. C.S.R. Matthes, N.M. Ghoniem, G.Z. Li, T.S. Matlock, D.M. Goebel, C.A. Dodson, and R.E. Wirz, "Fluence-Dependent Sputtering Yield of Micro-Architected Materials," *Appl. Surf. Sci.* **407**, pp 223-235 (2017).
4. A.J. Satonik, J.L. Rovey, and G. Hilmas, "Effects of Plasma Exposure on Boron Nitride Ceramic Insulators for Hall-Effect Thrusters," *J. Propulsion and Power* 30 (3), 656 (2014).
5. D.G. Zidar and J.L. Rovey, "Hall-Effect Thruster Channel Surface Properties Investigation," *J. Propulsion and Power* 28 (2), 334 (2012).
6. See <http://accuratus.com/alumox.html> for typical source material specifications.
7. M. Tartz, T. Heyn, C. Bundesmann, and H. Neumann, "Measuring Sputter Yields of Ceramic Materials," 31st International Electric Propulsion Conference, Paper IEPC-2009-240, Ann Arbor, Sept 2009.
8. J.T. Yim, M.L. Falk, and I.D. Boyd, "Modeling Low Energy Sputtering of Hexagonal Boron Nitride by Xenon Ions," *J. Appl. Phys.* 104, 123507 (2008).